

## Optical theorem for light scattering from a linear atomic chain

P. R. Berman \* and A. Kuzmich

Physics Department, University of Michigan, Ann Arbor, Michigan 48109-1040, USA



(Received 2 July 2021; accepted 15 October 2021; published 29 October 2021)

The radiation pattern of light scattered from a chain of atoms having  $J = 0$  ground states and  $J = 1$  excited states is calculated in the weak driving field approximation. It is shown that, in general, for arbitrary orientation of the driving field to the chain axis, it is not possible to treat the atoms in a two-level approximation owing to cooperative effects. In the limit of large detuning, however, all cooperative decay effects can be neglected in calculating the scattered spectrum. Nevertheless, even in this limit, in order to ensure conservation of energy, it is still necessary to include cooperative decay when calculating the energy lost by the *driving* field. For arbitrary detunings, conservation of energy can be expressed in the form of a generalized optical theorem.

DOI: [10.1103/PhysRevA.104.043714](https://doi.org/10.1103/PhysRevA.104.043714)

### I. INTRODUCTION

Light scattering of radiation by particles having dimensions much smaller than the wavelength of the radiation being scattered was analyzed in the pioneering work of Rayleigh [1]. An early discussion of light scattering by atoms can be found in the book by Heitler [2]. Both Rayleigh and Heitler understood that Rayleigh scattering is an elastic process and cannot be described, in general, as absorption and reemission by the scatterers. For weak incident fields, light scattering is essentially a two-photon process in which radiation from the incident field is scattered into previously unoccupied modes of the vacuum field. For stationary atoms (the only case considered in this work), the two-photon transition is between the same ground-state level—as a consequence the frequency of the scattered radiation is identical to that of the driving field. Heitler's calculation was carried out for the scattering of the incident field by a single atom, whereas Rayleigh considered independent scattering by an ensemble of dielectric spheres, allowing him to calculate an extinction coefficient.

The problem of light scattering by two atoms was discussed in a seminal paper by Richter using a two-level approximation [3]. A generalized theory of light scattering from regularly spaced atomic arrays in one, two, and three dimensions was given by Nienhuis and Schuller [4]. The modification of single-atom scattering resulting from a ground-state hyperfine structure has been considered by a number of authors [5–9]. Even for weak incident fields and a single ground-state level having total angular momentum  $J > 0$ , the scattering is no longer purely elastic, as it is for  $J = 0$  ground states. Müller *et al.* [9] went on to consider multiple scattering for these systems but adopted a model in which optical pumping and ground-state light shifts were neglected.

There has been a revival of interest in light scattering in the context of Bose condensates and quantum information.

For example, light scattering has been used to probe atomic interactions in Bose condensates [10]. Along with postselection, light scattering has also been used to create entangled states in atomic ensembles [11] which, in turn, could then be used in quantum information protocols. With an eye towards applications in quantum information, there have been studies of light scattering from linear atomic chains [12] and planar arrays [13].

Most treatments of light scattering by atomic chains are limited to or focused on situations in which the propagation vector of the incident field is either perpendicular or parallel to the axis chain. In such cases, the two-level approximation remains valid for a  $J = 0$  to  $J = 1$  transition. Scattering by a one-dimensional lattice of a field incident along the axis chain was studied experimentally by Glicenstein *et al.* [14], who found that the maximum scattered intensity as a function of the incident field frequency was red-shifted owing to atom-atom interactions.

In this paper we study light scattering from a one-dimensional chain of  $J = 0$  to  $1$  atoms for an arbitrary direction of the incident field propagation vector. Experimental studies of light scattering in this limit have revealed both Bragg scattering from a three-dimensional atomic lattice (that acted effectively as a one-dimensional regular array) [15] and reflective scattering from a one-dimensional atomic lattice [16]. In addition to obtaining the scattered intensity, we calculate the energy lost by the driving field in the scattering process, a subject that is not discussed in many of these previous studies. We show explicitly how the scattered intensity is equal to the rate at which energy is being depleted from the incident field by deriving an optical theorem for the scattering. As expected, we show that energy is conserved, but there is a novel aspect to the result. If the atom-field detuning is sufficiently large, all cooperative effects between the atoms can be neglected in calculating the scattered field. On the other hand, if we neglect cooperative decay in calculating the energy lost by the incident field in this limit, we get the wrong result. In other words cooperative decay can be neglected in calculating the scattered field for sufficiently large detunings but not for the energy loss of the incident field.

\*pberman@umich.edu

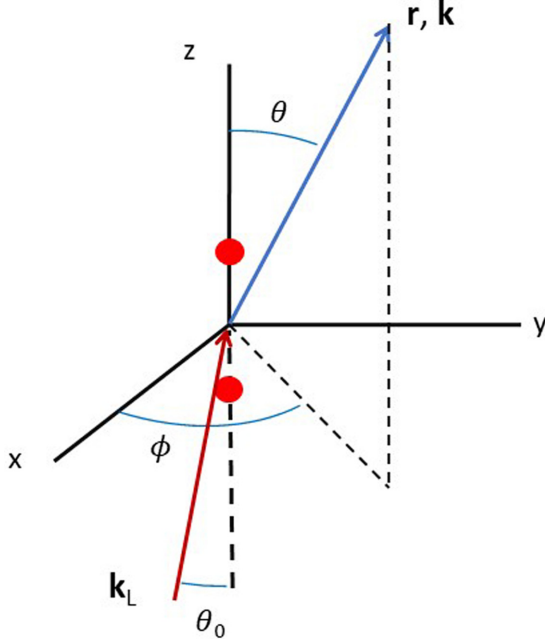


FIG. 1. Atom-field geometry. The propagation vector of the linearly polarized incident field lies in the  $x$ - $z$  plane and makes an angle  $\theta_0$  with the  $z$  axis. Two or more atoms are located on the  $z$  axis and scatter the incident radiation into a direction  $(\theta, \phi)$ .

## II. TWO ATOMS

To establish the notation and some of the concepts, we first consider scattering by two atoms. The atom-field geometry is indicated schematically in Fig. 1. Atom 1 is located at position  $\mathbf{R}_1 = -(Z_0/2)\mathbf{u}_z$  and atom 2 at position  $\mathbf{R}_2 = (Z_0/2)\mathbf{u}_z$ , with  $\mathbf{R}_{21} = \mathbf{R}_2 - \mathbf{R}_1 = Z_0\mathbf{u}_z$ , where  $\mathbf{u}_z$  is a unit vector. The incident field is taken to be a classical plane-wave field,

$$\mathbf{E}(\mathbf{R}, t) = \frac{1}{2}\epsilon_0 E_0 e^{i(\mathbf{k}_L \cdot \mathbf{R} - \omega_L t)} + \text{c.c.}, \quad (1)$$

where  $\omega_L = k_L c$  and “c.c.” stands for “complex conjugate.” The propagation vector

$$\mathbf{k}_L = k_L(\cos \theta_0 \mathbf{u}_z - \sin \theta_0 \mathbf{u}_x) \quad (2)$$

defines the plane of incidence and the polarization,

$$\epsilon = \cos \theta_0 \mathbf{u}_x + \sin \theta_0 \mathbf{u}_z, \quad (3)$$

is chosen to lie in this plane, although the calculation can be modified easily to allow for an arbitrary complex polarization (see the Appendix). Each atom has a  $J = 0$  ground state denoted  $g$  and a  $J = 1$  excited state denoted  $e$ . The transition frequency between the two levels is  $\omega_0$  and the excited-state decay rate is denoted  $\gamma_2$ .

The Hamiltonian for the atom-field system, written in a field-interaction representation within the rotating-wave approximation, is

$$H(t) = \frac{\hbar\delta}{2} \sum_{j=1,2} \sum_{m=-1}^1 \sigma_{mm}^{(j)} - \frac{1}{2} E_0 \sum_{j=1,2} \sum_{m=-1}^1 \mu_{mg} \cdot \epsilon e^{i\mathbf{k}_L \cdot \mathbf{R}_j} \tilde{\sigma}_{mg}^{(j)} - i \sum_{\mathbf{k}, \lambda} \left( \frac{\hbar\omega_k}{2\epsilon_0 V} \right)^{1/2}$$

$$\times \sum_{j=1,2} \sum_{m=-1}^1 \tilde{\sigma}_{mg}^{(j)} \mu_{mg} \cdot \epsilon_{\mathbf{k}}^{(\lambda)} a_{\mathbf{k}_k} e^{i\mathbf{k} \cdot \mathbf{R}_j} e^{-i(\omega_k - \omega_L)t} + \text{adjoint}, \quad (4)$$

where

$$\delta = \omega_0 - \omega_L \quad (5)$$

is the atom-field detuning,

$$\mu_{mg} = \langle m | \mu_j | g \rangle \quad (6)$$

is a ( $j$ -independent) dipole matrix element,  $|m\rangle$  is a ket corresponding to the  $m$  sublevel of the excited state,

$$\tilde{\sigma}_{mg}^{(j)}(t) = \sigma_{mg}^{(j)} e^{i\omega_L t}, \quad (7)$$

$\sigma_{mg}^{(j)}$  is a raising operator to state  $m$  in atom  $j$ ,  $\sigma_{mm}^{(j)}$  is an excited-state population operator for atom  $j$  in excited-state sublevel  $m$ ,  $a_{\mathbf{k}_k}$  is a lowering operator for the quantized field for a mode having propagation vector  $\mathbf{k} = k\hat{\mathbf{r}}$  and polarization

$$\epsilon^{(\theta)} = \cos \theta \cos \phi \hat{\mathbf{x}} + \cos \theta \sin \phi \hat{\mathbf{y}} - \sin \theta \hat{\mathbf{z}}, \quad (8a)$$

$$\epsilon^{(\phi)} = -\sin \phi \hat{\mathbf{x}} + \cos \phi \hat{\mathbf{y}}, \quad (8b)$$

$\omega_k = kc$ , and  $V$  is the quantization volume for the vacuum field.

The vacuum field leads to spontaneous decay of the excited states and coupling between the excited-state levels of one atom and those of the other. Explicitly, one can show that, owing to this coupling, the probability amplitudes  $c_{m;g}$  for atom 1 to be in state  $m$  and atom 2 to be in the ground state and  $c_{g;m}$  for atom 2 to be in state  $m$  and atom 1 to be in the ground state evolve as [4,17,18]

$$c_{g;m} = -\gamma c_{g;m} - \gamma(p_m + iq_m)c_{m;g}, \quad (9a)$$

$$\dot{c}_{m;g} = -\gamma c_{m;g} - \gamma(p_m + iq_m)c_{g;m}, \quad (9b)$$

where

$$p_{\pm 1}(\xi) = \frac{3}{2} \left\{ \frac{\sin \xi}{\xi} + \left( \frac{\cos \xi}{\xi^2} - \frac{\sin \xi}{\xi^3} \right) \right\}, \quad (10a)$$

$$q_{\pm 1}(\xi) = \frac{3}{2} \left\{ -\frac{\cos \xi}{\xi} + \left( \frac{\sin \xi}{\xi^2} + \frac{\cos \xi}{\xi^3} \right) \right\}, \quad (10b)$$

$$p_0(\xi) = -3 \left( \frac{\cos \xi}{\xi^2} - \frac{\sin \xi}{\xi^3} \right), \quad (11a)$$

$$q_0(\xi) = -3 \left( \frac{\sin \xi}{\xi^2} + \frac{\cos \xi}{\xi^3} \right), \quad (11b)$$

$$\gamma = \frac{\gamma_2}{2} = \frac{2}{3\sqrt{3}} \frac{\omega_L^3 \mu^2}{4\pi\epsilon_0 \hbar c^3}, \quad (12)$$

$$\xi = k_L R_{21} = k Z_0, \quad (13)$$

and  $\mu$  (assumed real) is the reduced matrix element of the dipole operator between the excited and the ground state. Since the atoms are on the  $z$  axis, the vacuum coupling is diagonal in the index  $m$ , but the coupling for  $m = 0$  states differs from that for  $m = \pm 1$  states. It has been assumed for simplicity that the shifts  $q_m$  are sufficiently small, that is, much less than  $\omega_0$ , to justify our use of the rotating-wave approximation. In addition, it has been assumed that  $\gamma R_{21}/c \ll 1$ ; otherwise

we would have to allow for the fact that  $\dot{c}_{g;m}(t)$  depends on  $c_{m;g}(t - R_{21}/c)$ .

There are two, independent complex decay parameters. In contrast, in a two-level approximation such as the one used by Richter, there is only a single linear combination

$$p_{\text{TL}}(\theta_0) = \frac{3}{2} \left\{ \cos^2 \theta_0 \frac{\sin \xi}{\xi} + \left( \frac{\cos \xi}{\xi^2} - \frac{\sin \xi}{\xi^3} \right) [1 - 3 \sin^2 \theta_0] \right\}, \quad (14a)$$

$$q_{\text{TL}}(\theta_0) = \frac{3}{2} \left\{ -\cos^2 \theta_0 \frac{\cos \xi}{\xi} + \left( \frac{\sin \xi}{\xi^2} + \frac{\cos \xi}{\xi^3} \right) [1 - 3 \sin^2 \theta_0] \right\}. \quad (14b)$$

Note that  $p_{\text{TL}}(0), q_{\text{TL}}(0) = p_{\pm 1}, q_{\pm 1}$  and  $p_{\text{TL}}(\pi/2), q_{\text{TL}}(\pi/2) = p_0, q_0$ , corresponding to polarization perpendicular and parallel to  $\hat{\mathbf{R}}_{21}$ .

### A. Scattered field intensity

The calculation of the scattered field intensity can now be carried out in a straightforward fashion. A convenient way to do this is to use source field theory [19]. The positive frequency of the field operator is written as

$$\mathbf{E}_+(\mathbf{r}, t) = \mathbf{E}_+^{(0)}(\mathbf{r}, t) + \mathbf{E}_+^{(\text{Source})}(\mathbf{r}, t), \quad (15)$$

where  $\mathbf{E}_+^{(0)}(\mathbf{r}, t)$  is the field operator in the absence of the source atoms and  $\mathbf{E}_+^{(\text{Source})}(\mathbf{r}, t)$  is the field operator associated with the sources. If the input field is a coherent state, the operator  $\mathbf{E}_+^{(0)}(\mathbf{r}, t)$  can be replaced by its classical counterpart,  $\frac{1}{2}\epsilon E_0 e^{i(\mathbf{k}_L \cdot \mathbf{r} - \omega_L t)}$ . Moreover, in calculating the scattered field intensity for a  $J = 0$  to  $J = 1$  transition, it is possible to replace the source field operator by its average value, provided saturation effects can be neglected [8].

As a consequence, we can write the total average field as

$$\langle \mathbf{E}_+(\mathbf{r}, t) \rangle = \frac{1}{2} \epsilon E_0 e^{i(\mathbf{k}_L \cdot \mathbf{r} - \omega_L t)} + \langle \mathbf{E}_+^{(\text{Source})}(\mathbf{r}, t) \rangle, \quad (16)$$

where  $\langle \mathbf{E}_+^{(\text{Source})}(\mathbf{r}, t) \rangle$  in the radiation zone, as calculated from Eq. (19.68) in Ref. [19], is given by

$$\begin{aligned} \langle \mathbf{E}_+^{(\text{Source})}(\mathbf{r}, t) \rangle &= \text{sgn}(\mu) \sqrt{\hbar \omega_0 \gamma_2} \sqrt{\frac{3}{16\pi \epsilon_0 c}} \frac{e^{i(k_L R - \omega_L t)}}{R} \\ &\times \sum_{j=1,2} \sum_{m=-1}^1 \sum_{\lambda=\theta,\phi} e^{-i\mathbf{k} \cdot \mathbf{R}_j} P_m^{(\lambda)}(\theta, \phi) \epsilon^{(\lambda)} \langle \tilde{\sigma}_{gm}^{(j)} \rangle, \end{aligned} \quad (17)$$

with

$$P_m^{(\theta)}(\theta, \phi) = - \left( \frac{e^{i\phi} \delta_{m,1} - e^{-i\phi} \delta_{m,-1}}{\sqrt{2}} \right) \cos \theta - \delta_{m,0} \sin \theta, \quad (18a)$$

$$P_m^{(\phi)}(\theta, \phi) = \frac{i}{\sqrt{2}} (e^{i\phi} \delta_{m,1} + e^{-i\phi} \delta_{m,-1}), \quad (18b)$$

and

$$\mathbf{k} = k_L \hat{\mathbf{r}}. \quad (19)$$

of magnetic substates excited by the classical field in atom 1 and this linear combination is coupled to the *same* linear combination in atom 2. For the atom-field geometry of this problem, the values of  $p$  and  $q$  in the two-level approximation are

The differential scattered field intensity in each of the polarization modes is calculated as

$$I_\theta(\hat{\mathbf{r}}) = 2\epsilon_0 c R^2 \left| \langle \mathbf{E}_+^{(\text{Source})}(\mathbf{r}, t) \rangle \cdot \epsilon^{(\theta)} \right|^2, \quad (20a)$$

$$I_\phi(\hat{\mathbf{r}}) = 2\epsilon_0 c R^2 \left| \langle \mathbf{E}_+^{(\text{Source})}(\mathbf{r}, t) \rangle \cdot \epsilon^{(\phi)} \right|^2, \quad (20b)$$

and the total differential scattered intensity is

$$I(\hat{\mathbf{r}}) = I_\theta(\hat{\mathbf{r}}) + I_\phi(\hat{\mathbf{r}}). \quad (21)$$

The problem reduces to solving for the  $\langle \tilde{\sigma}_{gm}^{(j)} \rangle$  for  $j = 1, 2$ . From the Hamiltonian, (4), it follows that the evolution equations of these quantities are

$$d\langle \tilde{\sigma}_{gm}^{(1)} \rangle / dt = -(\gamma + i\delta) \langle \tilde{\sigma}_{gm}^{(1)} \rangle - \gamma(p_m + iq_m) \langle \tilde{\sigma}_{gm}^{(2)} \rangle - S_{1m}, \quad (22a)$$

$$d\langle \tilde{\sigma}_{gm}^{(2)} \rangle / dt = -(\gamma + i\delta) \langle \tilde{\sigma}_{gm}^{(2)} \rangle - \gamma(p_m + iq_m) \langle \tilde{\sigma}_{gm}^{(1)} \rangle - S_{2m}, \quad (22b)$$

where

$$S_{jm} = i\chi f_m e^{i\mathbf{k}_L \cdot \mathbf{R}_j}, \quad (23)$$

$$f_m = - \left( \frac{\delta_{m,1} - \delta_{m,-1}}{\sqrt{2}} \right) \cos \theta_0 + \delta_{m,0} \sin \theta_0, \quad (24)$$

and

$$\chi = - \frac{\mu E_0}{2\sqrt{3}\hbar} \quad (25)$$

is (one) half of an effective Rabi frequency associated with the incident field-atom interaction. Retardation times corresponding to the time it takes for light propagation between the atoms have been neglected under the assumption that  $\gamma Z_0/c \ll 1$ .

Equations (22) are solved easily at steady state to yield

$$\langle \tilde{\sigma}_{gm}^{(1)} \rangle = -i\chi f_m e^{i\mathbf{k}_L \cdot \mathbf{R}_1} A_m / \gamma, \quad (26a)$$

$$\langle \tilde{\sigma}_{gm}^{(2)} \rangle = -i\chi f_m e^{i\mathbf{k}_L \cdot \mathbf{R}_2} B_m / \gamma, \quad (26b)$$

where

$$A_m = \frac{1}{2} \left[ \frac{1 + e^{i\mathbf{k}_L \cdot \mathbf{R}_{21}}}{(1 + p_m) + i(\delta/\gamma + q_m)} + \frac{1 - e^{i\mathbf{k}_L \cdot \mathbf{R}_{21}}}{(1 - p_m) + i(\delta/\gamma - q_m)} \right], \quad (27a)$$

$$B_m = \frac{1}{2} \left[ \frac{1 + e^{-i\mathbf{k}_L \cdot \mathbf{R}_{21}}}{(1 + p_m) + i(\delta/\gamma + q_m)} + \frac{1 - e^{-i\mathbf{k}_L \cdot \mathbf{R}_{21}}}{(1 - p_m) + i(\delta/\gamma - q_m)} \right]. \quad (27b)$$

Note that  $A_1 = A_{-1}$ . Combining Eqs. (20), (17), and (26), we then find that the differential scattered intensity for each polarization may be written as

$$I_\lambda(\hat{\mathbf{r}}) = \frac{3}{8\pi} \hbar \omega_L \gamma_2 \frac{|\chi|^2}{\gamma^2} \left| \sum_{m=-1}^1 P_m^{(\lambda)}(\theta, \phi) f_m (A_m + e^{i(\mathbf{k}_L - \mathbf{k}) \cdot \mathbf{R}_{21}} B_m) \right|^2 \quad (\lambda = \theta, \phi), \quad (28)$$

and the total scattered intensity as

$$\begin{aligned} I &= \int I(\hat{\mathbf{r}}) d\Omega = \int [I_\theta(\hat{\mathbf{r}}) + I_\phi(\hat{\mathbf{r}})] d\Omega \\ &= \hbar \omega_L \gamma_2 \frac{|\chi|^2}{\gamma^2} \sum_{m=0}^1 f_m^2 \left[ \frac{(1 + p_m)(1 + \cos \alpha)}{[(1 + p_m)^2 + (\delta/\gamma + q_m)^2]} + \frac{(1 - p_m)(1 - \cos \alpha)}{[(1 - p_m)^2 + (\delta/\gamma - q_m)^2]} \right], \end{aligned} \quad (29)$$

with

$$\alpha = k_L Z_0 \cos \theta_0. \quad (30)$$

These solutions agree with those of the two-level approximation [3] for  $\theta_0 = 0$  or  $\pi/2$  but not for arbitrary  $\theta_0$ .

In Fig. 2, the dimensionless total differential scattered intensity (solid red curve)

$$I_N(\theta, \phi) = \frac{8\pi \gamma^2}{3\hbar \omega_L \gamma_2 |\chi|^2} I(\hat{\mathbf{r}}) = \frac{8\pi \gamma^2}{3\hbar \omega_L \gamma_2 |\chi|^2} [I_\theta(\hat{\mathbf{r}}) + I_\phi(\hat{\mathbf{r}})] \quad (31)$$

is plotted as a function of  $\theta$  for  $\theta_0 = 0.5$ ,  $\delta/\gamma = 1$ ,  $k_L Z_0 = 1$ , and  $\phi = 0$ . The dashed blue curve is the two-level approximation result for these parameters and the dotted black curve is twice the dimensionless intensity scattered by a single atom. In Fig. 3, the dimensionless total scattered intensity

$$I_N = \frac{\gamma^2}{\hbar \omega_L \gamma_2 |\chi|^2} I \quad (32)$$

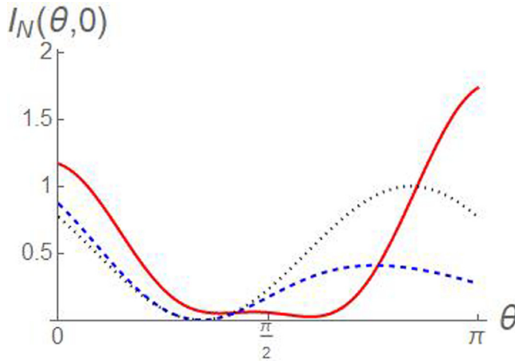


FIG. 2. Graphs of the dimensionless differential scattered intensity as a function of  $\theta$  for  $\theta_0 = 0.5$ ,  $\delta/\gamma = 1$ ,  $k_L Z_0 = 1$ , and  $\phi = 0$ . The solid red curve is our result, the dashed blue curve is the two-level result, and the dotted black curve is (twice) the single-atom result.

is plotted as a function of  $\delta/\gamma$  for  $\theta_0 = 0.5$  and  $k_L Z_0 = 1$  (solid red curve). The dashed blue curve is the two-level approximation result for these parameters. In our expression for  $I$ , there are two pairs of resonances at  $\delta = \pm\gamma q_1, \pm\gamma q_0$ , whereas the two-level approximation theory predicts a *single* pair of resonances at  $\delta = \pm\gamma q_{\text{TL}}(\theta_0)$ . For example, if  $\theta_0 = 0.5$ , we find resolved resonances at  $\delta = \pm 1.3\gamma, \pm 4.2\gamma$ , whereas the two-level approximation theory predicts unresolved resonances at  $\delta = \pm 0.02\gamma$ . The resonances are evident in Fig. 3. Note that the maximum value of  $I_N$  in these units for two noninteracting atoms is equal to 2 for  $\delta = 0$ , obtained by setting  $p_m = q_m = 0$  in Eq. (29). By plotting  $I_N(\delta = 0)$ , given by Eqs. (32) and (29), as a function of  $k_L Z_0$  and  $\theta_0$ , it can be shown that an upper bound for  $I_N(\delta = 0)$  is 2.24, occurring for  $(\theta_0 = 0, k_L Z_0 = 5.0)$ , whereas the upper bound in the two-level approximation result is 3.07, occurring for  $(\theta_0 = 0.527, k_L Z_0 = 0.729)$ . Figures 2 and 3 provide clear evidence for the breakdown of the two-state approximation. If we had taken  $\theta_0 = 0$  and  $\phi = 0$ , the maximum differential scattered intensity would occur at  $\theta = 0, \pi$ , while for  $\theta_0 = \pi/2$  and  $\phi = 0$ , it occurs at  $\theta = \pi/2$ ; in both these limits,

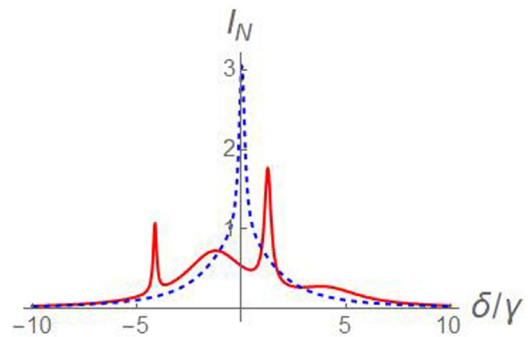


FIG. 3. Graphs of the dimensionless total scattered intensity as a function of  $\delta/\gamma$  for  $\theta_0 = 0.5$  and  $k_L Z_0 = 1$ . The solid red curve is our result and the dashed blue curve is the two-level result.

the two-level approximation is valid. The value  $\theta_0 = 0.5$  has been chosen somewhat at random to illustrate the differences between the exact results and those corresponding to the two-level approximation.

An interesting limit is  $|\delta| \gg \gamma q_1, \gamma q_0, \gamma$  (note that to have  $|\delta|/\gamma \gg q_1, q_0$ , it is necessary that  $\xi^{-3} \ll |\delta|/\gamma$ ). In that limit cooperative effects play no role, the two-level approximation is valid, and

$$I(\hat{\mathbf{r}}) \sim [2s(\hat{\mathbf{r}})] \frac{3}{8\pi} \hbar \omega_L \gamma_2 \frac{|\chi|^2}{\delta^2} \{1 + \cos [(\mathbf{k}_L - \mathbf{k}) \cdot \mathbf{R}_{21}]\}, \quad (33a)$$

$$I \sim 2\hbar \omega_L \gamma_2 \frac{|\chi|^2}{\delta^2} [1 + p_{\text{TL}}(\theta_0) \cos \alpha], \quad (33b)$$

where

$$s(\hat{\mathbf{r}}) = 1 - (\boldsymbol{\epsilon} \cdot \hat{\mathbf{r}})^2 = 1 - (\cos \theta_0 \sin \theta \cos \phi + \sin \theta_0 \cos \phi)^2 \quad (34)$$

is the (dimensionless) differential scattering cross section of a single atom and  $p_{\text{TL}}(\theta_0)$  is given by Eq. (14a). When  $\xi = k_L Z_0 \ll 1$  (but still greater than  $[\gamma/|\delta|]^{1/3}$ ), the radiation pattern  $I(\hat{\mathbf{r}})$  is essentially the same as the single-atom radiation pattern but with four times the intensity. The total scattered intensity  $I$  is also four times that of a single atom. On the other hand, for  $\xi \gg 1$ , the radiation pattern has superimposed on it a number of Bragg maxima and minima, with the Bragg maxima having four times the intensity of single-atom emission. In this case, when integrated over solid angle, the combined maxima and minima lead to a total scattered intensity that is approximately equal to twice that of a single atom.

Since we have assumed that  $|\delta| \gg \gamma q_1, \gamma q_0, \gamma$  to arrive at Eq. (33b), cooperative effects play no role in this result. Nevertheless, the cooperative decay scaling parameter  $p_{\text{TL}}(\theta_0)$ , defined in Eq. (14a), appears in Eq. (33b). It has arisen from the integration over solid angle and *not* from any inclusion of cooperative decay. The total scattered intensity reflects the fact that there can be constructive or destructive interference of the radiation scattered by the two atoms as a function of the scattering angle, even if atom-atom interactions are neglected. A complementary process occurs in the emission pattern from two phased dipoles [20]. In that case, the correct phase-matched emission can be calculated neglecting cooperative decay if the atoms are separated by greater than a wavelength. However, there is a problem with energy conservation; the total energy radiated in all directions is greater or less than the energy stored originally in the atoms. It is necessary to include modifications of the dipole decay rates resulting from cooperative emission to restore conservation of energy. In the scattering problem considered in this work, we also run into a problem with energy conservation—that is, if cooperative decay is neglected, the scattered radiation energy is not equal to the energy lost by the driving field. To restore energy conservation, it is necessary to include cooperative decay when calculating the energy lost by the driving field. It is to such a calculation that we now turn our attention.

## B. Energy lost by the incident field

Within this source field approach it is a simple matter to calculate the energy lost by the field. It follows from Eq. (16) for the average field amplitude that the total intensity is given by

$$I_{\text{tot}} = I_0 + I + I_x, \quad (35)$$

where  $I_0$  is the intensity of the incident field,  $I$  is the intensity of the scattered field given by Eq. (29), and

$$I_x = \epsilon_0 c R^2 E_0 e^{-i\omega_L t} \lim_{R \rightarrow \infty} R^2 \int d\Omega e^{i\mathbf{k}_L \cdot \mathbf{r}} \langle \mathbf{E}_+^{(\text{Source})}(\mathbf{r}, t) \rangle \cdot \boldsymbol{\epsilon} + \text{c.c.} \quad (36)$$

We can write  $\langle \mathbf{E}_+^{(\text{Source})}(\mathbf{r}, t) \rangle$  in the form

$$\langle \mathbf{E}_+^{(\text{Source})}(\mathbf{r}, t) \rangle = \frac{k_L R}{4\pi} \frac{e^{i(k_L R - \omega_L t)}}{R^2} \mathbf{G}_+^{(\text{Source})}(\theta, \phi, t), \quad (37)$$

where

$$\mathbf{G}_+^{(\text{Source})}(\theta, \phi, t) = \frac{4\pi}{k_L} \text{sgn}(\mu) \sqrt{\hbar \omega_0 \gamma_2} \sqrt{\frac{3}{16\pi \epsilon_0 c}} \sum_{j=1}^2 \sum_{m=-1}^1 \times \sum_{\lambda=\theta, \phi} e^{-i\mathbf{k} \cdot \mathbf{R}_j} P_m^{(\lambda)}(\theta, \phi) \boldsymbol{\epsilon}^{(\lambda)} \langle \tilde{\sigma}_{gm}^{(j)} \rangle. \quad (38)$$

From Eqs. (36) and (37), it can be seen that the integrand in the expression for  $I_x$  contains an exponential factor,

$$\exp [i\{k_L R[1 - (\cos \theta_0 \cos \theta - \sin \theta_0 \sin \theta \cos \phi)]\}],$$

that is rapidly varying in all but the  $\mathbf{k}_L$  direction ( $\theta = \theta_0$ ,  $\phi = \pi$ ). As a consequence all terms in the integrand can be evaluated at ( $\theta = \theta_0$ ,  $\phi = \pi$ ), except for terms appearing in this lead exponential. The integral over the solid angle can then be performed easily if the  $z$  axis is redefined along the  $\mathbf{k}_L$  direction, such that the exponential factor reduces to  $\exp[i[k_L R(1 - \cos \theta)]]$  and

$$\lim_{R \rightarrow \infty} \frac{k_L R}{4\pi} \int d\Omega \exp [i\{k_L R(1 - \cos \theta)\}] = -\frac{1}{2i}, \quad (39)$$

leading to

$$I_x = -\text{Im} [\epsilon_0 c E_0 \mathbf{G}_+^{(\text{Source})}(\theta_0, \pi, t) \cdot \boldsymbol{\epsilon}], \quad (40)$$

which is an expression of the optical theorem for this problem. Using Eqs. (40), (17), (18), (26), (3), (12), (24), and (25), we obtain

$$I_x = -\hbar \omega_L \gamma_2 \frac{|\chi|^2}{2\gamma^2} \sum_{m=0}^1 f_m^2 [(A_m + B_m) + \text{c.c.}] \quad (41)$$

In the limit that cooperative effects are negligible,

$$[(A_m + B_m) + \text{c.c.}] \sim \frac{4}{1 + (\delta/\gamma)^2}, \quad (42)$$

implying that

$$I_x \sim -2\hbar \omega_L \gamma_2 \frac{|\chi|^2}{\gamma^2 + \delta^2}, \quad (43)$$

twice the single-atom result. Equation (43) is *not* consistent with Eq. (33b), which was derived neglecting cooperative effects but allowed for interference effects between the radiation

scattered from the two atoms. In other words, in the limit that cooperative effects can be neglected, the expressions for  $I_x$  and  $I$  do not satisfy energy conservation since  $I_x \neq -I$ . On the other hand, if we include cooperative effects,

$$I_x \approx -\hbar\omega_L\gamma_2 \frac{|\chi|^2}{\gamma^2} \sum_{m=0}^1 f_m^2 \left[ \frac{(1+p_m)(1+\cos\alpha)}{[(1+p_m)]^2 + (\delta/\gamma+q_m)^2} + \frac{(1-p_m)(1-\cos\alpha)}{[(1-p_m)]^2 + (\delta/\gamma-q_m)^2} \right], \quad (44)$$

consistent with Eq. (29) for any value of  $\delta/\gamma$ .

### III. GENERALIZATION TO $N$ ATOMS ON A LINE

It is not overly difficult to extend the calculation to one in which there are  $N$  atoms located at positions  $\mathbf{R}_j = Z_j \mathbf{u}_z$ . Equations (22) are replaced by

$$\begin{aligned} d\langle\tilde{\sigma}_{gm}^{(j)}\rangle/dt &= -(\gamma + i\delta)\langle\tilde{\sigma}_{gm}^{(j)}\rangle \\ &\quad - \gamma \sum_{j' \neq j=1}^N [p_m(\xi_{jj'}) + iq_m(\xi_{jj'})]\langle\tilde{\sigma}_{gm}^{(j')}\rangle \\ &\quad - i\chi f_m e^{i\mathbf{k}_L \cdot \mathbf{R}_j}, \end{aligned} \quad (45)$$

where  $\xi_{jj'} = k_L|Z_j - Z_{j'}|$ ,  $p_m(\xi_{jj'})$ , and  $q_m(\xi_{jj'})$  are given in Eqs. (10) and (11), and  $j$  runs from 1 to  $N$ . It is convenient to set

$$\langle\tilde{\sigma}_{gm}^{(j)}\rangle = -i\chi f_m \gamma b_m^{(j)} e^{i\mathbf{k}_L \cdot \mathbf{R}_j}, \quad (46)$$

where the  $N$ -dimensional vector  $\mathbf{b}_m$  having components  $b_m^{(j)}$  satisfies the vector differential equation

$$d\mathbf{b}_m/dt = -\Gamma_m \mathbf{b}_m + \mathbf{1}, \quad (47)$$

in which  $\Gamma_m$  is an  $N \times N$  matrix having elements

$$(\Gamma_m)_{jj} = 1 + i\delta/\gamma, \quad (48a)$$

$$(\Gamma_m)_{jj'} = [p_m(\xi_{jj'}) + iq_m(\xi_{jj'})]e^{-ik_L Z_{jj'} \cos\theta}; \quad j \neq j'. \quad (48b)$$

The steady-state solution of Eq. (47) for the components of  $\mathbf{b}_m$  is

$$b_m^{(j)} = \sum_{j'=1}^N [(\Gamma_m)^{-1}]_{jj'}. \quad (49)$$

The calculation then proceeds as in the two-atom case and we find a differential scattered field intensity,

$$I_\lambda(\hat{\mathbf{r}}) = \frac{3}{8\pi} \hbar\omega_L\gamma_2 \left| \frac{\chi}{\gamma} \right|^2 \left| \sum_{m=-1}^1 P_m^{(\lambda)}(\theta, \phi) f_m \sum_{j=1}^N F^{(j)}(\theta) b_m^{(j)} \right|^2, \quad (50)$$

$$I(\hat{\mathbf{r}}) = I_\theta(\hat{\mathbf{r}}) + I_\phi(\hat{\mathbf{r}}), \quad (51)$$

where

$$F^{(j)}(\theta) = e^{-ik_L Z_j (\cos\theta - \cos\theta_0)}$$

and  $P_m^{(\lambda)}$  is defined in Eqs. (18). It is possible to carry out the integration over the solid angle to obtain the total scattered

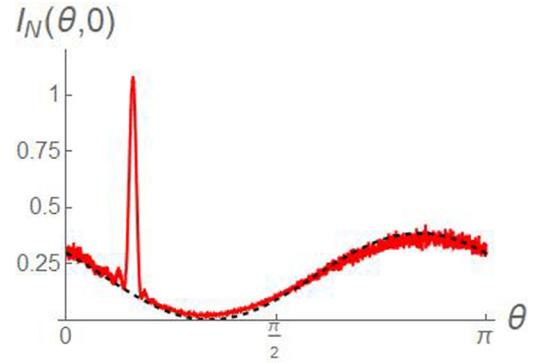


FIG. 4. Dimensionless differential scattered intensity as a function of  $\theta$  for  $\delta/\gamma = 5$ ,  $\phi = 0$ ,  $\theta_0 = 0.5$ , and 10 atoms placed at random positions on a line having length  $L = 200/k_L$ . The curve corresponds to an average over 400 trials. The dashed black curve is 10 times the single-atom scattered intensity.

intensity,

$$I = \hbar\omega_L\gamma_2 \frac{|\chi|^2}{\gamma^2} \sum_{m=-1}^1 f_m^2 \sum_{j, j'=1}^N p_m(\xi_{jj'}) e^{ik_L Z_j \cos\theta_0} b_m^{(j)} [b_m^{(j')}]^*. \quad (52)$$

For detunings much larger than any decay rates or shifts,

$$I(\hat{\mathbf{r}}) \sim \frac{3}{8\pi} s(\hat{\mathbf{r}}) \hbar\omega_L\gamma_2 \frac{|\chi|^2}{\delta^2} S \quad (53)$$

and

$$I \sim \hbar\omega_L\gamma_2 \frac{|\chi|^2}{\delta^2} \left[ N + 2p_{TL}(\theta_0) \sum_{j, j'=1}^N \sum_{j' < j} \cos(\mathbf{k}_L \cdot \mathbf{R}_{jj'}) \right], \quad (54)$$

where the structure factor  $S$  is defined by

$$S = \left| \sum_{j'=1}^N \exp\{i \cos[(\mathbf{k}_L - k_L \hat{\mathbf{r}}) \cdot \mathbf{R}_{jj'}]\} \right|^2. \quad (55)$$

The same procedure can be used to calculate the energy lost by the field. The only difference is that the sum over  $j$  in Eq. (38) now goes from 1 to  $N$ . Using Eqs. (40), (38), (25), (12), (3), (8), and (46), we find that

$$I_x \approx -\hbar\omega_L\gamma_2 \frac{|\chi|^2}{\gamma^2} \text{Im} \left[ i \sum_{m=-1}^1 f_m P_m^{(\lambda)}(\theta_0, \pi) \sum_{j=1}^N b_m^{(j)} \right], \quad (56)$$

which is a statement of the optical theorem for the ensemble of scatterers. It has been assumed that any propagation effects can be neglected; that is, the incident field is assumed to propagate through the medium without distortion and the energy lost to scattering represents a small fraction of the energy in the pulse. We have verified numerically that  $I_x$ , as given by Eq. (56), is the negative of the scattered intensity  $I$  given by Eq. (52).

In Fig. 4, we plot the dimensionless total differential scattered intensity as a function of  $\theta$  for  $\delta/\gamma = 5$ ,  $\phi = 0$ ,  $\theta_0 = 0.5$ , and 10 atoms placed at random positions on a line having length  $L = 200/k_L$ . The curve corresponds to an average over 400 trials. For these parameters the average spacing of the

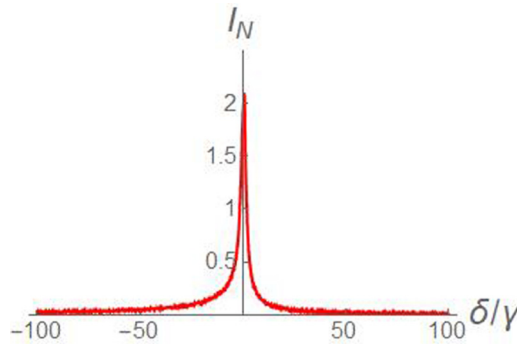


FIG. 5. Dimensionless total scattered intensity as a function of  $\delta/\gamma$  for  $\theta_0 = 0.5$  and 10 atoms placed at random positions on a line having length  $L = 5/k_L$ . The curve corresponds to an average over 400 trials.

atoms is  $Z_{\text{avg}} = 20/k_L$ . Since  $k_L Z_{\text{avg}} = 20$ , cooperative effects play a minor role, but the interference from different atoms leads to numerous resonance peaks. On averaging over many trials, however, the only resonance that remains is for phase-matched reflection with  $\theta = \theta_0$ , as found experimentally by Tamura *et al.* [16]. The dashed black curve is 10 times the single-atom scattered intensity. At  $\theta = \theta_0$  the scattered phase-matched intensity is approximately 94 times that of a single atom (it is slightly less than 100 owing to the fact that cooperative effects are not *totally* negligible, even with an average spacing of  $20/k_L$ ). In Fig. 5, we plot the dimensionless total scattered intensity as a function of  $\delta/\gamma$  for the same parameters, except the length, which is now taken as  $L = 5/k_L$ , where cooperative effects play a role ( $k_L Z_{\text{avg}} = 0.5$ ). The wings of this curve, extending well beyond  $|\delta/\gamma| = 1$ , arise from the cooperative shifts. Owing to the fact that the shifts  $q_{\pm 1}$ , which are positive for  $k_L R_{jj'} \lesssim 1$ , are weighted more heavily for  $\theta_0 = 0.5$  than the negative shifts,  $q_0$ , there is an overall asymmetry in this curve favoring negative values of  $\delta$ . This asymmetry would be more severe if we had chosen  $\theta_0 = 0$  since the cooperative shifts at small separation are positive, whereas the asymmetry would be reversed if we had  $\theta_0 = \pi/2$  since the cooperative shifts at small separation are negative. Moreover, the peak of the curve is shifted slightly to the blue for the same reason, in contrast to the red shift that would occur for  $\theta_0 = 0$ , as found by Glicenstein *et al.* [14].

#### IV. SUMMARY

We have developed a formalism that allows us to calculate the intensity of radiation scattered by a linear chain of atoms,

including cooperative decay. We have shown that a generalization of the optical theorem holds for the scattering; that is, the total energy scattered by the atoms is related to the average forward scattered field amplitude. If both the scattered intensity and energy lost by the field are calculated neglecting cooperative effects, there is a violation of energy conservation. To restore energy conservation in this limit, corrections to the energy lost by the field must be included to lowest order in the cooperative effects. Although the calculation was limited to 10 atoms, it is generalized easily to any number of atoms. The calculation can also be generalized to atoms placed in a two- or three-dimensional array. In that case, it is necessary to use a more general approach to consider cooperative effects, in which the cooperative coupling of the excited-state magnetic sublevels is no longer diagonal in the index  $m$  [18]. For level schemes involving a higher angular momentum, optical pumping must be taken into account. Even for the simple atom-field geometry studied in this work and for a  $J = 0$  to  $J = 1$  transition, we have shown that a two-level approximation, sometimes employed by other authors, is not valid for arbitrary directions of the incident field.

#### ACKNOWLEDGMENTS

This research was supported by the AFOSR and the National Science Foundation.

#### APPENDIX: ARBITRARY POLARIZATION

The calculation is generalized easily to allow for arbitrary polarization of the input field,

$$\epsilon = \beta_{\parallel}(\cos \theta_0 \hat{x} - \sin \theta_0 \hat{z}) + \beta_{\perp} \hat{y}, \quad (\text{A1})$$

where  $\beta_{\parallel}$  and  $\beta_{\perp}$  are arbitrary complex numbers satisfying

$$|\beta_{\parallel}|^2 + |\beta_{\perp}|^2 = 1. \quad (\text{A2})$$

The only change in the calculation is that the quantities  $f_m$  given in Eq. (24) are now replaced,

$$f_m = -\left(\frac{\delta_{m,1} - \delta_{m,-1}}{\sqrt{2}}\right)\beta_{\parallel} \cos \theta_0 + \delta_{m,0}\beta_{\parallel} \sin \theta_0 + i\left(\frac{\delta_{m,1} + \delta_{m,-1}}{\sqrt{2}}\right)\beta_{\perp}, \quad (\text{A3})$$

and  $f_m^2$  is replaced by  $|f_m|^2$  wherever it appears.

---

- [1] L. Rayleigh, *Philos. Mag.* **47**, 375 (1899).
- [2] W. Heitler, *The Quantum Theory of Radiation*, 3rd ed. (Oxford, UK, 1954), Sec. 20.
- [3] Th. Richter, *Opt. Acta* **30**, 1769 (1983).
- [4] G. Nienhuis and F. Schuller, *J. Phys. B* **20**, 23 (1987).
- [5] D. Polder and M. F. H. Schurmans, *Phys. Rev. A* **14**, 1468 (1976).
- [6] J. Javanainen, *Europhys. Lett.* **20**, 395 (1992).
- [7] B. Gao, *Phys. Rev. A* **50**, 4139 (1994).
- [8] P. R. Berman, *Contemp. Phys.* **49**, 313 (2008).
- [9] C. A. Müller, C. Miniatura, D. Wilkowski, R. Kaiser, and D. Delande, *Phys. Rev. A* **72**, 053405 (2005).
- [10] See, for example, D. Stamper-Kurn and W. Ketterle, *Les Houches Summer School Session LXXII*, edited by R. Kaiser, C. Westbrook, and F. David (Springer, New York, 2001), pp. 137.

- [11] L.-M. Duan, M. D. Lukin, J. I. Cirac, and P. Zoller, *Nature (London)* **414**, 413 (2001); for a review, see N. Sangouard, C. Simon, H. de Riedmatten, and N. Gisin, *Rev. Mod. Phys.* **83**, 33 (2011).
- [12] For a review with many references, see L. A. Williamson and J. Ruostekoski, *Phys. Rev. Research* **2**, 023273 (2020).
- [13] See, for example, C. Weitenberg, P. Schauß, T. Fukuhara, M. Cheneau, M. Endres, I. Bloch, and S. Kuhr, *Phys. Rev. Lett.* **106**, 215301 (2011).
- [14] A. Glicenstein, G. Ferioli, N. Šibalić, L. Brossard, I. Ferrier-Barbut, and A. Browaeys, *Phys. Rev. Lett.* **124**, 253602 (2020).
- [15] S. Slama, C. von Cube, A. Ludewig, M. Kohler, C. Zimmermann, and Ph. W. Courteille, *Phys. Rev. A* **72**, 031402(R) (2005).
- [16] H. Tamura, H. Nguyen, P. R. Berman, and A. Kuzmich, *Phys. Rev. Lett.* **125**, 163601 (2020).
- [17] D. A. Hutchinson and H. F. Hameka, *J. Chem. Phys.* **41**, 2006 (1964).
- [18] H. Fu and P. R. Berman, *Phys. Rev. A* **72**, 022104 (2005).
- [19] See, for example, P. R. Berman and V. S. Malinovsky, *Principles of Laser Spectroscopy and Quantum Optics* (Princeton University Press, Princeton, NJ, 2011), Chap. 19.
- [20] P. R. Berman, *Am. J. Phys.* **78**, 1323 (2010).